MAGNETO-ACOUSTIC EMISSION FOR THE CHARACTERISATION OF FERRITIC STAINLESS STEEL STRESS STATE

D. O'Sullivan[1], M. Cotterell[1], S. Cassidy[1], D.A. Tanner[2] and I. Mészáros[3]

1. Department of Mechanical and Manufacturing Engineering, Cork Institute of Technology, Bishopstown, Cork, Ireland. Email: dosullivan@cit.ie
2. Department of Materials Science and Technology, University of Limerick, Limerick, Ireland.
3. Budapest University of Technology and Economics, Department of Materials Science and Engineering, H-1111 Goldmann ter 3, (V2/159), Budapest, Hungary.

KEY WORDS: magneto-acoustic emission, ferritic stainless steel, residual stress

ABSTRACT

The role of residual stresses in the failure of metallic components and the need to determine such stresses is well recognised. Magneto-acoustic emission (MAE) is a relatively new non-destructive detection technique and its working principle is based on Barkhausen discontinuities or noise and magnetostriction when a ferromagnetic material is subjected to a varying magnetic field. MAE is being used to characterise the stress state of a ferritic stainless steel (AISI 430). Other stress measurement techniques; X-ray diffraction (XRD), magnetic Barkhausen noise (MBN) have also been used to confirm / support the results achieved using MAE. A new measurement parameter has been developed for stress characterisation called MAE absolute energy and has proved to be a useful quantitative method in MAE waveform measurement. I can't seem to get to grips with this last sentence. When you say stress characterisation, what do you mean?

1. INTRODUCTION

High stress corrosion resistance and relatively low production costs are the main reasons for the increasing applications of AISI 430 ferritic stainless steels [1]. But problems such as loss of ductility and toughness when exposed to elevated temperatures, for instance during welding, is a main concern [2]. The heat of welding leads to grain coarsening in the heat effected zone and in the weld metal of ferritic stainless steels because they solidify directly from the liquid to the ferrite phase without any intermediate phase transformation [2-3]. The use of a non-destructive evaluation technique to characterise the post-welding microstructural state of a material, could be of use in determining the optimal levels of heat input and welding speeds.

For characterisation, ferritic stainless steel (AISI 430) samples were plastically deformed and heat treated to various degrees and measured using Barkhausen sensing techniques. In a ferromagnetic material, Barkhausen noise (BN) is generated by the discontinuous movement of irreversible domains walls. This movement can be induced by applying a time varying magnetic field across the sample. This noise can be detected in the form of acoustic noise (electrical energy) or in the form of voltage pulses which are induced in a coil placed near the surface of the material. Magnetic Barkhausen noise (MBN) results from the reversible and irreversible displacement of 180º and non-180º domain walls, or by abrupt rotation of domain magnetisation vectors at higher magnetic fields. Acoustic Barkhausen noise, measured by magneto-acoustic

emission (MAE), is only caused by the discontinuous motion of non-180° walls, or the irreversible rotation of domains through angles other than 180° [4-6]. This is because 180° walls are not associated with stress, and non-180° walls are [7]. It is the acoustic pulses given out by the generation of stresses from the movement of non-180° walls that are detected and analysed. No stresses are generated as a result of 180º wall motion or rotation because the strain along a particular axis is independent of the direction of magnetic moments if they lie along the axis.

Barkhausen noise can also be affected by pinning sites which act as barriers to domain movement. Pinning sites are attributed to various physical parameters such as grain boundaries, voids, inclusions and dislocations.

Amongst the wide range of techniques available for NDT evaluation of stresses, magnetic Barkhausen noise measurement has become very popular for stress analysis. Macroscopic magnetic properties such as differential permeability are well known to be stress-dependent [8]. The stress-dependence of differential permeability carries through to micro-scale effects to cause MBN also to be stress-dependent [9-10].

But the significance of MAE for the detection of stresses in ferromagnetic materials has received little attention. MAE has not yet been used for industrial purposes, and it is hoped that the results presented here will help to further advance this technique for its use as a non-destructive evaluation of stress.

The main difference between the two Barkhausen techniques is the measurement depth. The depth of the measurement depends on the frequency of the excitation, but typically for MBN is in the range of 0.1-1mm (surface measurement) and for MAE between 0-10mm (bulk measurement) depending on the permeability of the material.

2. EXPERIMENTAL METHOD

Flat specimens have been cut from a sheet of AISI 430. Could you mention what temper you received the material in? I see on the Matweb site that it mentions several different types!!!!! Others won't be able to repeat if they use different grade / temper. For instance, I would love to know if it had been rolled or underwent a gross deformation process before you received it – this could be relevant to the results that you have presented. The as-received chemical composition of the material included 14.19% Cr, 0.9% Mn, 84.91% Fe. All tensile samples have been prepared in accordance to [11]. These samples were deformed to various degrees of strain within the plastic range (i.e. from the yield point of the material to the ultimate tensile strength point.). Standardised test specimen dimensions (120mmx10mmx1.5mm) were used as outlined in [11], and strain was measured using an extensometer with a gauge length of 50mm which was calibrated according to [11]. Tensile tests were completed on seven samples to determine yield point and ultimate tensile strength of the specimens.

Samples plastically strained to 17.5% were subjected to annealing heat treatment for the purpose of stress relief. Heat treatments were completed for 100ºC to 1100ºC with a soaking time of 30 minutes. Samples removed from the furnace were air-cooled.

Seven specimens were elongated at each plastic strain percentage. Five measurements of each measurement technique were completed on each specimen across the surface. The standard deviation of the results from each specimen was then calculated using conventional formulae.

2.1. Barkhausen measurement

2.2.1. Magnetic Barkhausen noise (MBN)

The magnetic Barkhausen noise utilised a sinusoidal (10 Hz) exciting magnetic field produced by a function generator and a power amplifier. The applied measuring head contained a U-shaped magnetising coil and a pick-up coil, which is perpendicular to the surface of the specimen. The signal of the pick-up coil was processed by a 0.3 kHz-38 kHz band pass filter and amplified with a gain of 50. A National Instruments data acquisition card (PCI-6023) with a sampling rate of 200kS/s was utilised. LabVIEW was used for processing the noise signal. The applied sampling frequency was 100 kHz and the maximum magnetic field induction of the excitation was 20 gauss. The Root Mean Square (RMS) value of the noise signal was determined and was used to characterise the microstructural state of the material.

2.2.2. Magneto-acoustic emission (MAE)

A U-shaped electromagnet was used to apply a time varying magnetic field (sinusoid @ 10Hz) across the samples to achieve magnetic domain rotation. The acoustic emission sensor was coupled to the surface of the specimens using Vaseline BP white petroleum jelly. The couplant insures good surface contact between the two surfaces on a microscopic level and aids the transmittal of acoustic waves between the two surfaces. The MAE sensing head was applied to the surface of the specimens, where the AE (acoustic emission) sensor had a spring back force of 15N and the electromagnet had an application force of 25N. A total preamplifier gain of 60dB (x1000) was used for signal amplification before it was measured with a digital oscilloscope. All MAE waveforms were collected using a Tektronix TDS 220 digital storage oscilloscope, which has a sampling rate of 1GS/s. The magnetic field strength used for the excitation was 35kA/m.

<u>Absolute energy</u>

A method to determine the area of the waveform was derived called the MAE absolute energy. Acoustic emission (AE) can be defined as the transient elastic waves resulting from localised internal micro-displacements taking place in a solid. The AE consists of bursts of energy, which can vary in amplitude over several orders of magnitude. When this occurs within a material, the piezoelectric AE sensor is excited by the stress waves impinging on its face. This mechanical signal is converted to an electrical signal by the piezoelectric device. AE energy is the measured energy of an electrical waveform, which is the result of a mechanical excitation of a piezoelectric sensor. Thus since the MAE waveform is an energy signal, it is characterised by the area under the waveform over a fixed period.

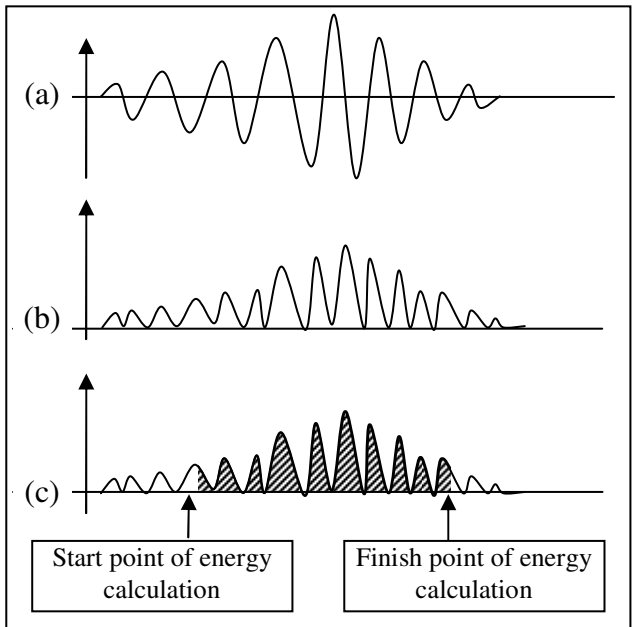

Figure 1. Absolute energy measurement (a) waveform, (b) absolute waveform and (c) MAE energy calculation.

The first step in the absolute energy calculation process is the acquisition of the AE signal by the system (figure 1(A)). The signal

waveform is then rectified (figure 1(B)) or made absolute so that all negative peaks become positive. Each voltage received is evaluated and the total absolute energy for that signal is determined (figure 1(C)). This can be seen as an accurate method of evaluating the energy of a signal as the energy is directly related to the piezoelectric crystal.

The area of the MAE signal was calculated by taking each consecutive pair of data points and calculating the area between these points using geometrical techniques from the algorithm developed as shown below.

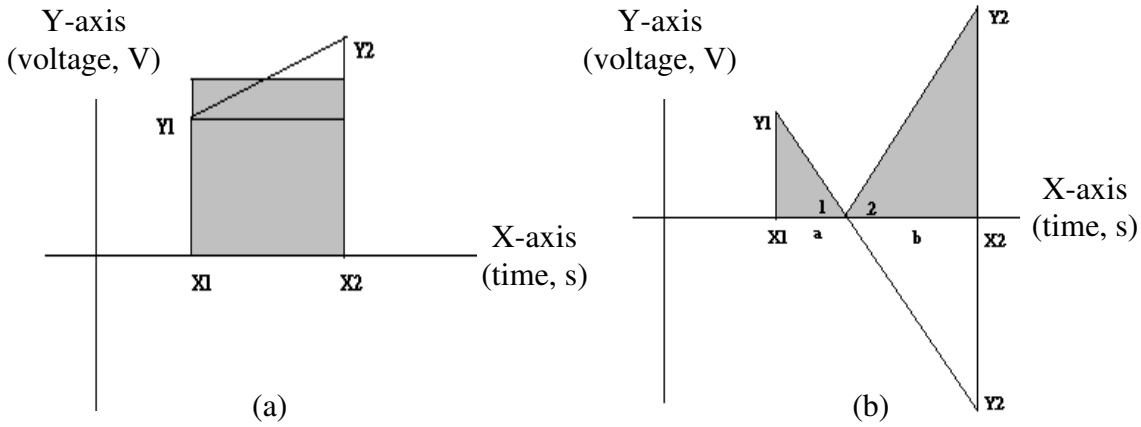

Figure 2. (a) both Y Cartesian coordinates are of same polarity, (b) consecutive points of opposite polarity.

When both points Y1 and Y2 are of the same polarity (either both +ve or both -ve)(figure 2(a)), the area was calculated by using [EQN. 1]:

[EQN. 1] $$Area = (X2 - X1) * \left(\frac{(Y1 + Y2)}{2} \right)$$

Could you use subscripte (X_1, X_2) It would just make it easier to understand the above diagram?

When the points Y1 or Y2 are of opposite polarity, because the absolute area has to be calculated, therefore the negative Y value has to be made absolute to become a positive value and then the area between the two points was calculated using [EQN. 2 and EQN. 3]:

[EQN. 2] $$Area = \left(\frac{Y1}{2} \right)\left((X2 - X1) - b\right) + \left(\frac{Y2}{2} \right)(b)$$

[EQN. 3] $$\text{where } b = \frac{(X2 - X1)(Y2)}{(Y1 + Y2)}$$

By using either of these two methods to calculate the area between the points the total area under the graph can be calculated. An executable MS DOS program was developed and used to calculate the absolute energy. Absolute energy is given in arbitrary units. I don't see how it has arbitrary units seen as it is obtained by multiplying X by Y giving units of V.s?

2.2.3. Barkhausen noise signal

A typical waveform output from the MAE sensor can be seen below. The excitation signal is shown as the sinusoidal waveform, and the resultant MAE waveform is also shown. As can be seen in figures 3(a) and 3(b), the MAE signal reduces with increased material deformation.

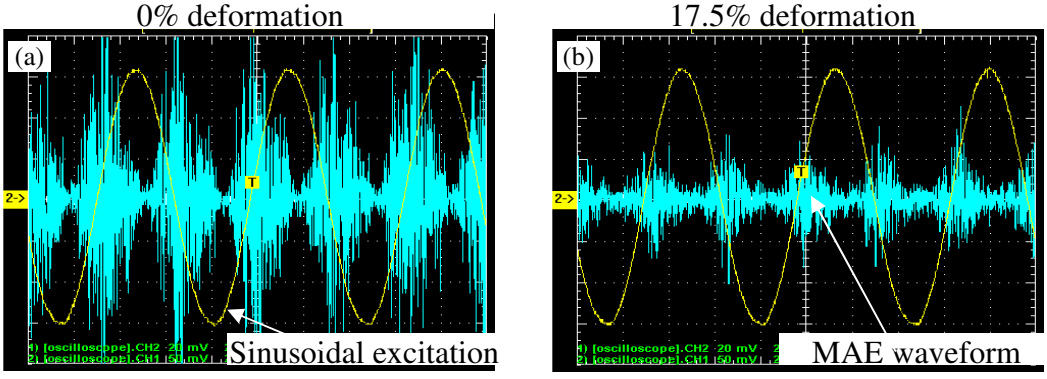

Figure 3. Shows the resultant MAE signal from (a) no deformation and (b) 17.5% plastically deformed AISI 430 samples. I understand that this figure shows the difference between the deformed samples but there is no scale on either axis? I take it that the yellow line (which won't print out in B & W) is on the same scale on both plots – you should mention this somewhere.

2.2. Microhardness

Vickers hardness (HV) measurements were completed using a Buehler MMT-3 digital microhardness tester. All tests were completed using a load of 2000 gf (19614mN) according to [12].

2.3. X-ray diffraction

Uniaxial residual stress magnitudes were determined using the local strain x-ray diffraction technique (XRD) as outlined in literature [13-16]. Residual stress was determined at the center of one surface of tensile samples strained to 17.5% one of which was in the as strained condition, one heat treated at 700°C and one heat treated at 1100°C, using a Philips X'Pert x-ray diffractometer.

Scan parameters were controlled using Philips X'Pert Data Collector (V1.2a) software with 2θ values (2θ – angle between source and diffracted x-ray beam) chosen to encompass the Cu-Kα doublet for the {222} planes: $135° \leq 2\theta \leq 138.5°$. A minimum of twelve scans were performed for each measurement using evenly distributed ψ angles within the range $0 \leq \psi \leq 60°$ (ψ – angle between the surface normal and the bisector of source and diffracted x-ray beam). Only positive tilting was used as negative tilting can lead to poor quality peaks when using the ω-diffraction geometry [14].

The resulting spectra were analysed using Philips X'Pert Stress Software [17]. The $Sin^2\psi$ technique was used with a $\frac{1}{2}S_2$ value of $5.21 \times 10^{-12}(m^2/N)$ taken from literature for the {222} plane [13]. The Pearson VII technique was used to calculate the peak position on the diffracted intensity plots [18]. The measurements taken indicated that the lattice spacing d versus $Sin^2(\psi)$ plots were linear, confirming that texture and stress gradient did not affect the calculated stress magnitudes. Shearing stresses were assumed negligible when compared with normal stress magnitudes. The errors quoted are fit errors of the d versus $Sin^2(\psi)$ plots calculated by the software. This software allowed a misalignment calculation to be performed confirming that the specimen height and machine alignment was correct even though specimen height has not been found to have a large effect on determined stress magnitudes [14].

2.4. Microstructural Analysis

For microstructural examination, the etching of the ferritic AISI 430 stainless steel was carried out using swab etching with a solution of HCL, HNO_3 and H_2O with a ratio of 1:1:1. The etching time varied between 4–8 minutes. The revealed microstructure can be seen in figures 6(b), 6(c) and 6(d). The grain size G, was calculated according to [19] and was used as a measurand to analyse the deformed microstructure, post elongation.

3. RESULTS

The dependence of MAE absolute energy and MBN (RMS) on the deformation of AISI 430 ferritic stainless steel is shown in figures 4 and 6.

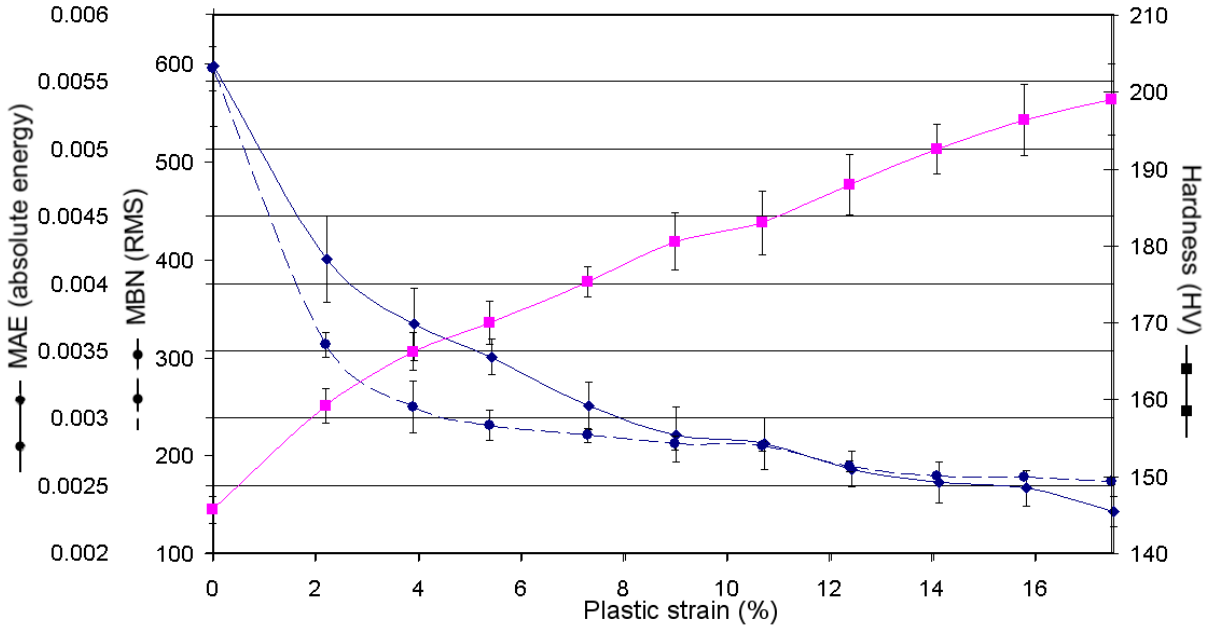

Figure 4. Dependence of MAE, MBN and hardness on percentage plastic strain for AISI 430. *I still can't tell these apart when I print them out. Same goes for Figure 6.*

It can be seen at the lowest level of plastic strain 0% (as-received condition), where no permanent deformation of the material has occurred, the MAE and MBN are seen to be at their highest (figure 4). With increased straining, both the MAE and MBN continuously reduce.

It is known that as plastic deformation increases, the dislocation density increases, and that a change in the arrangement of dislocations in the specimen occurs as indicated by transmission electron microscopy [20]. The magnetic domain walls get pinned or held in place by dislocation interactions. Because of increased domain-wall dislocation interactions at increased plastic deformation, the magnetising force is not high enough to set them free and reduced domain movement results in decreased BN [21]. This also results in increased hardening of the material with increased strain.

Figure 5 shows that the inverse of MAE (absolute energy) and MBN (RMS) are linearly proportional to hardness, i.e. an increase plastic strain with a corresponding increase in hardness, results in a decrease in MAE and MBN.

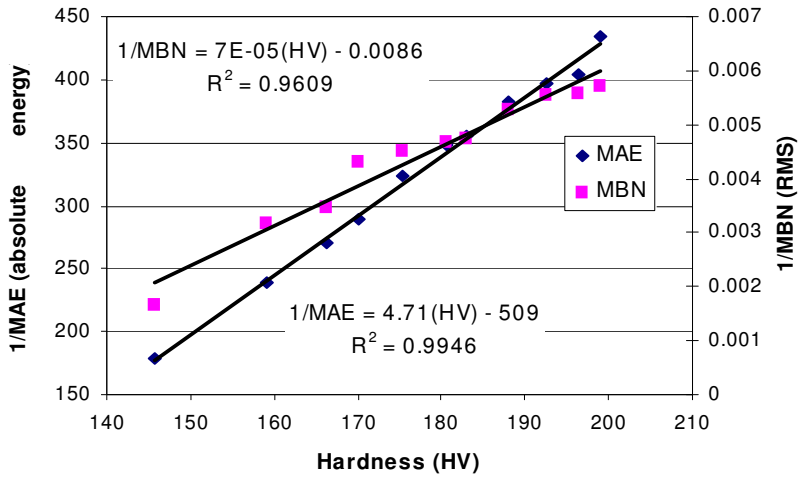

Figure 5. The relationship between hardness and the inverse of MAE and MBN for AISI 430.

Figure 6 shows the effect of annealing on hardness, MAE and MBN. An examination of the plot shows that the BN has low level energy between 100º to about 500ºC where the material is in its hardest state. This would correspond to the high dislocation density levels within the material and associated domain-wall

interactions. The slight increase in the MBN measurement at 300ºC was due to superfluous material distortion brought about during material preparation.

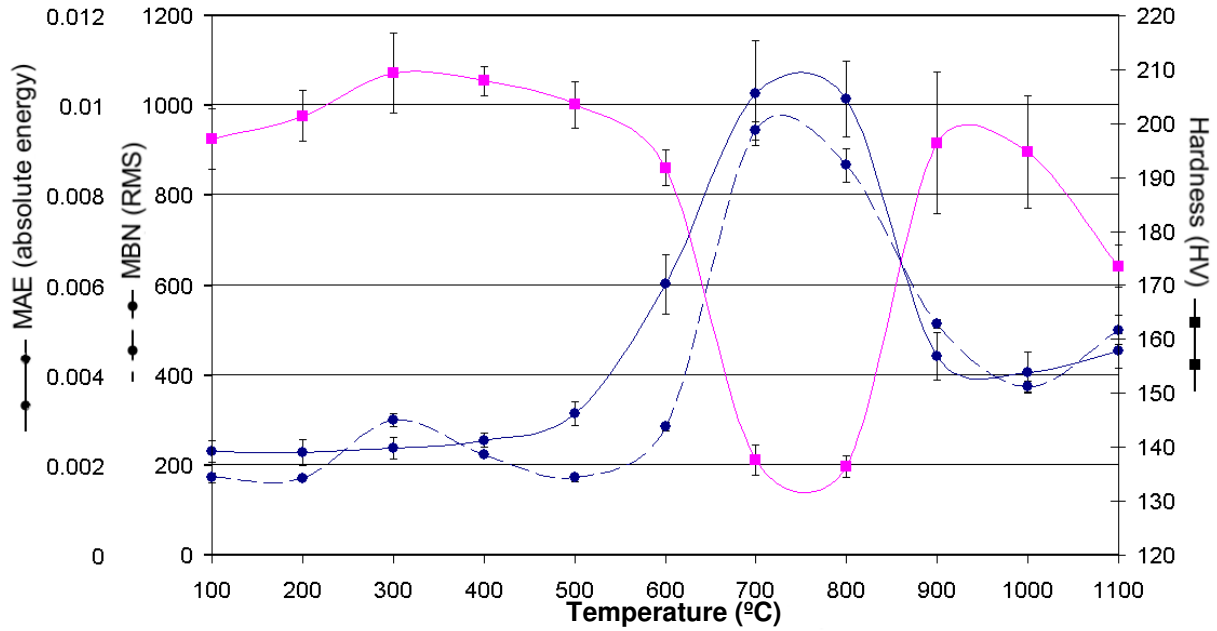

Figure 6. MAE, MBN and hardness as a function of heat treatment temperature for AISI 430.

Above this temperature, the BN increases. The annealing of the material can be seen to begin at 600ºC from the hardness measurements. The recovery process of the dislocations in which they begin to rearrange themselves occurs here. As a result, the small change in hardness can be attributed to this rearrangement and a small reduction in the density of dislocations. But it is between 700-800ºC that the material is fully annealed. This is where the minimum hardness and maximum ductility, toughness, and corrosion resistance of the material occurs. Thus the domain wall-dislocation interactions are at their lowest, leading to greater BN.

The increase in hardness above 800ºC occurs because of austenite-martensite embrittlement. Because these samples were cooled in air, they become brittle due to small volumes of austenite transforming to martensite [22]. This can be seen from the microstructural examination in figure 7(d). The martensite phase has a high dislocation density which increases the barriers to domain wall movement, thus reducing the Barkhausen noise. At elevated temperatures the recovery process continues and decreased material strength is observed with corresponding increased BN.

In both the plastically strained and heat-treated results, the MBN measurements indicate that the surface of the specimens have a slightly higher stress than the bulk of the specimens at certain strains and heat treatment temperatures. Throughout experimentation, the results from both Barkhausen techniques are seen to compare favourably.

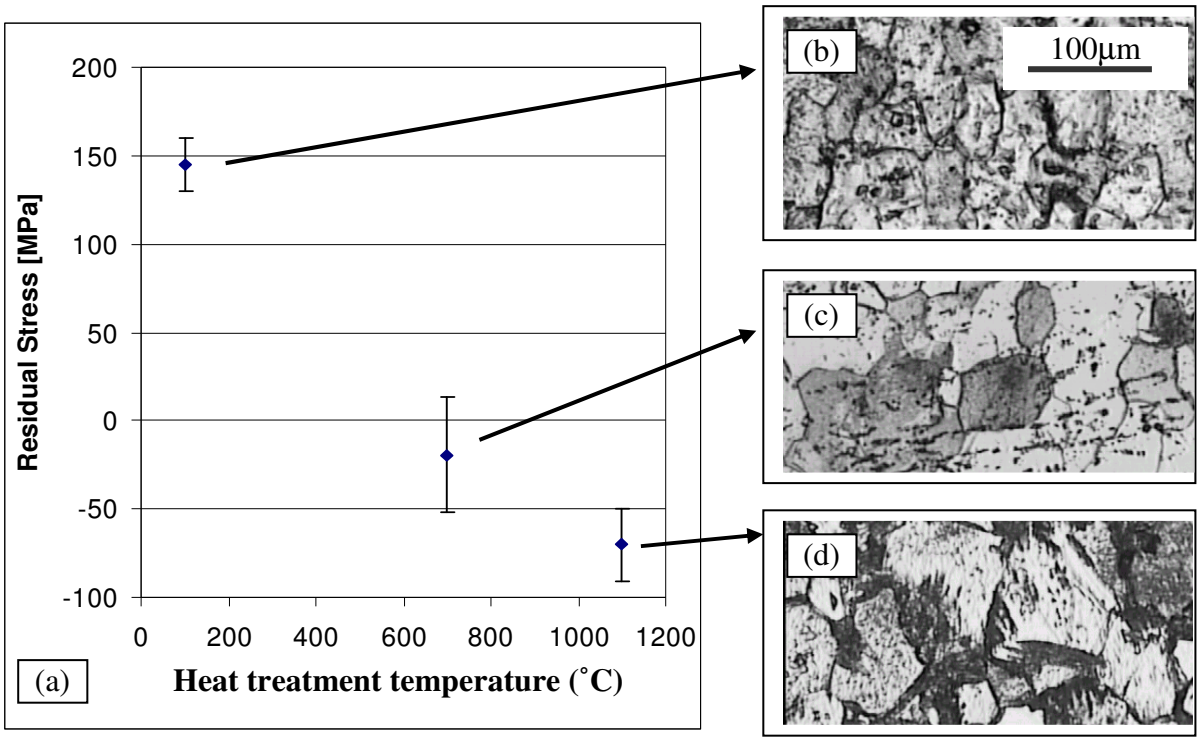

Figure 7. (a) XRD residual stress results on heat-treated samples, (b) deformed microstructure (ASTM G = 7.23), (c) annealed (ASTM G = 6.04) and (d) austenite-martensite embrittlement (ASTM G = 5.64).

XRD residual stress measurements were completed on the surface of the heat treated samples (figure 7(a)). This technique was used to verify the findings of the BN measurements. At 100ºC, in the deformed grain structure (prior to annealing), the residual stresses were found to be tensile and relatively high. And as expected, a decrease in the stresses at the annealing temperature (700ºC) was observed i.e. post annealing (as-received grain structure). The increase in the martensitic phase at 1100ºC, which is larger in volume than the host austenite phase resulted in compressive stresses of the material.

4. CONCLUSION

Magneto-acoustic emission was used to characterise the microstructural state of ferritic stainless steel. It was found that:

- MAE absolute energy was found to be linearly inversely proportional to hardness.
- In both the plastically strained and heat-treated samples, the MBN and MAE measurements are seen to be comparable.
- XRD measurements and microstructural observations have been completed on the samples and validate BN measurements.
-
- MAE and MBN can be used as an effective means for ferritic stainless steel microstructural characterisation.

I really wouldn't use shorthand in the conclusions – sometimes people will only read them.

5. ACKNOWLEDGEMENTS

The authors gratefully acknowledge financial assistance for this project provided by Enterprise Ireland under the International Collaboration Fund, and to the assistance from the University of Limerick and the Budapest University of Technology and Economics.

6. REFERENCES

[1] W.S. Brandão, V.T.L. Buono, P.V. Marques, and P.J. Modenesi, *Welding Int*., vol. 6 (1992), 713.
[2] V.T.L. Buono, B.M. Gonzalez and M.S. Andrade, Strain aging of AISI 430 ferritic stainless steel, *Scripta Materialia*, Vol. 38 (1998), No. 2, 185-190.
[3] T. Mohandas, G. Madhusudhan Reddy, Mohammad Naveed, A comparative evaluation of gas tungsten and shielded metal arc welds of a 'ferritic' stainless steel. *Journal of Materials Processing Technology*, Vol. 94 (1999),133-140.
[4] H. Kusanagi, H. Kimura, and H.S. Sasaki, *J. Appl. Phys*., Vol. 50 (1976), 2985
[5] S. Tyagi, J. Steinberg, A.E. Lord, Jr., and P.M. Anderson, *Phys. Status Solidi*, Vol. 64 (1984), 443.
[6] M. M. Kwan, K. Ono, and M. Shibata, *J. Acoust. Emission*, Vol. 3 (1984), 144.
[7] D. C. Jiles, *Introduction to Magnetism and Magnetic Materials*, Chapman and Hall, 1991.
[8] D. C. Jiles and D.L. Atherton, Theory of the magnetisation process in ferromagnets and its application to the magnetomechanical effect. *J. Phys. D: Appl. Phys*., Vol. 17 (1984), No. 6, 1265-1281
[9] M.J. Sablik, *J. Applied Phys*., Vol. 74 (1993), 5899
[10] M.J. Sablik and B. Augustyniak, *J. Appl. Phys*., Vol. 79 (1996), 963.
[11] BS EN 10 002-1:1990, 'Tensile testing of metallic materials'.
[12] ASTM E 384-99, 'Standard test method for microindentation hardness of materials'.
[13] V. Hauk: *Adv in Sur Treat, Technol - Appl - Eff.*, 1987, **4**, 251-302.
[14] M. E. Fitzpatrick, A. T. Fry, P. Holdway, F. A. KandilL, J. Shackleton and L. Suominen: 'Determination of residual stresses by X-ray diffraction. Measurement and Practice Guide'; 2002, NPL
[15] P. S. Prevey: In *Metals Handbook,* Vol. 10 (Ed, Mills, K.), 1986, OH, American Society for Metals, 380-392.
[16] I. C. Noyan and J. B. Cohen: In *Residual Stress [Measurement by Diffraction and Interpretation],* 1987, New York, Springer-Verlag.
[17] Philips X'Pert Stress. 1.0a, 2001, Philips Analytical B.V.
[18] M. M. Hall Jr, V. G. Veeraraghavan, H. Rubin and P. G. Winchell: *Journal Applied Crystallography*, 1977, 10, 66-68.
[19] ASTM E112-96 standards, 'Standard Test Methods for Determining Average Grain Size'.
[20] L. Burkhardt, R.E. Beissner, G.A. Matzkanin, and J.D. King. Acoustic methods for obtaining Barkhausen noise stress measurements, *Materials Evaluation*, Vol. 40 (1981), 669-675.
[21] Buttle, D.J., Scruby C.B., Briggs, G.A.D., E.A. Little and Jakubovics, J.P. Magnetoacoustic and Barkhausen emission in ferromagnetic materials. Phil. Trans. R. Soc. Lond. A320, 1986, pp. 363-378.
[22] ASM Handbook, Metallography and Microstructure, Vol. 9, 1988.